RADIATION RESEARCH **181**, 177–183 (2014)
0033-7587/14 $15.00

DOI: 10.1667/RR13464.1

The Effects of Ultra-High Dose Rate Proton Irradiation on Growth Delay in the Treatment of Human Tumor Xenografts in Nude Mice

O. Zlobinskaya,[a] C. Siebenwirth,[b] C. Greubel,[b] V. Hable,[b] R. Hertenberger,[c] N. Humble,[a] S. Reinhardt,[c] D. Michalski,[a] B. Röper,[a] G. Multhoff,[a] G. Dollinger,[b] J. J. Wilkens[a] and T. E. Schmid[a,1]

[a] *Department of Radiation Oncology, Klinikum rechts der Isar, Technische Universität München, München, Germany;* [b] *Institut für Angewandte Physik und Messtechnik (LRT2), Universität der Bundeswehr München, Neubiberg, Germany; and* [c] *Ludwig-Maximilians-Universität München, Fakultät für Physik, Garching, Germany*

Zlobinskaya, O., Siebenwirth, C., Greubel, C., Hable, V., Hertenberger, R., Humble, N., Reinhardt, S., Michalski, D., Röper, B., Multhoff, G., Dollinger, G., Wilkens, J. J. and Schmid, T. E. The Effects of Ultra-High Dose Rate Proton Irradiation on Growth Delay in the Treatment of Human Tumor Xenografts in Nude Mice. *Radiat. Res*. 181, 177–183 (2014).

The new technology of laser-driven ion acceleration (LDA) has shown the potential for driving highly brilliant particle beams. Laser-driven ion acceleration differs from conventional proton sources by its ultra-high dose rate, whose radiobiological impact should be investigated thoroughly before adopting current clinical dose concepts. The growth of human FaDu tumors transplanted onto the hind leg of nude mice was measured sonographically. Tumors were irradiated with 20 Gy of 23 MeV protons at pulsed mode with single pulses of 1 ns duration or continuous mode (~100 ms) in comparison to controls and to a dose-response curve for 6 MV photons. Tumor growth delay and the relative biological effectiveness (RBE) were calculated for all irradiation modes. The mean target dose reconstructed from Gafchromic films was 17.4 ± 0.8 Gy for the pulsed and 19.7 ± 1.1 Gy for the continuous irradiation mode. The mean tumor growth delay was 34 ± 6 days for pulsed, 35 ± 6 days for continuous protons, and 31 ± 7 days for photons 20 ± 1.2 Gy, resulting in RBEs of 1.22 ± 0.19 for pulsed and 1.10 ± 0.18 for continuous protons, respectively. In summary, protons were found to be significantly more effective in reducing the tumor volume than photons ($P < 0.05$). Together with the results of previous *in vitro* experiments, the *in vivo* data reveal no evidence for a substantially different radiobiology that is associated with the ultra-high dose rate of protons that might be generated from advanced laser technology in the future.

INTRODUCTION

Radiotherapy with charged particles has attracted a lot of interest over the last years due to the superior dose distribution of protons and heavy ions (*1*). Laser technology is evolving very quickly, and dedicated groups, mainly in the U.S., Europe and Japan, are exploring the potential of high-intensity ultra-short laser pulses to accelerate ion beams (*2–4*). Potential advantages of laser-driven particle therapy arise from combining a compact, cost-efficient treatment unit with the physical advantages in dose delivery of charged particle beams (*5*).

One of the key differences with regard to radiobiological effects of laser-accelerated particles versus conventionally accelerated particles that utilize cyclotrons or synchrotrons is that laser-driven particle beams are delivered in ultra-short pulses. While the duration of laser pulses that is required for the acceleration of particles to MeV energies is in the range of femtoseconds, the resulting particle pulse will spread in time during beam transport. Subsequently, nanosecond particle pulses will be obtained. It is expected that a tissue voxel exposed to this kind of radiotherapy will receive a substantial part of the full dose from a few nanosecond pulses (resulting dose rate $\geq 10^9$ Gy/s) (*6*). In contrast, conventional proton irradiation in a synchrotron or cyclotron delivers the same dose over a time period of milliseconds to seconds. These data reveal differences in the peak dose rate of 6–9 orders of magnitude. Thus, before utilization of a laser-driven proton therapy in a clinical setting, it is crucial to understand whether an ultra-high dose rate alters any relevant biological endpoints.

As a surrogate for a laser-driven proton beam, the experiments were performed with the scanning ion microprobe SNAKE [Superconducting Nanoscope for Applied Nuclear (Kern) Physics Experiments] (*7*) at the Munich tandem accelerator. Until recently, the SNAKE has been limited in beam energy and repetition rate, allowing for cell experiments only (*6*) however with recent updates SNAKE is now available for animal studies. Utilization of SNAKE, allows direct comparisons between protons of ultra-high dose rate and continuous irradiation schemes to

[1] Addresss for correspondence: Klinikum rechts der Isar, Department of Radiation Oncology, Technische Universität München, Ismaningerstr. 22, München, Bavaria 81675, Germany; e-mail: t.e.schmid@lrz.tu-muenchen.de.

be made. For the latter, a continuous and defocused proton beam was used where the dose of a few Gy is deposited within the millisecond range.

A series of experiments exploring DNA repair, cytogenetic damage and cell death as endpoints has already been performed in monolayer cell cultures (*in vitro*) using the ultra-high dose-rate effects of protons produced by the SNAKE. With respect to these endpoints no indication for a significantly altered efficiency of pulsed protons compared to a continuous irradiation was observed (*8–11*). Further biological experiments were performed using a human skin tissue model to account for the 3D geometry and the cell interaction, again without statistically significant changes in RBE according to dose rate (*12*). In addition to these *in vitro* studies, a technical set-up for *in vivo* irradiation of subcutaneous tumors in mice with pulsed and continuous proton beams has now been constructed at the SNAKE (*13*).

The aim of the current study was to investigate the tumor growth delay in mice that are induced by 23 MeV protons at pulsed versus continuous irradiation mode in comparison to 6 MV photons.

MATERIALS AND METHODS

Cell Lines and Culture Conditions

FaDu (*14, 15*) a human hypopharyngeal squamous cell carcinoma line (ATCC HTB-43) was kindly provided by Prof. Baumann (Dresden, Germany). Cells were cultured in Dulbecco's modified Eagle's medium (DMEM) (Invitrogen) containing 10% fetal calf serum (FCS), 0.05 mg/ml penicillin, 0.05 mg/ml streptomycin, 2% Hepes, 1% nonessential amino acids, 1% sodium-pyruvate and maintained in a humidified atmosphere of 95% air and 5% CO_2 at 37°C.

Animals and Tumor Model

All experiments were performed using 7- to 10-week-old female NMRI (nu/nu) mice (Charles River Laboratories, Germany) according to German federal law and with approval of the regional animal ethics committee (project license 55.2-1-54-2531-37-09). Exponentially growing FaDu cells were inoculated in the axilla of mice (1×10^6 cells in 200 µl NaCl). Tumors of 5 mm diameter were excised, cut in 1 mm^3 pieces and frozen in 10% dimethylsulfoxide (DMSO) and 90% FCS in liquid nitrogen. Two weeks before irradiation FaDu tumor pieces were implanted subcutaneously in the hind legs of the mice. The implantation incisions were sealed with Histoacryl® Topical Skin Adhesive (Braun Biosurgicals, Germany). Three days before transplantation the mice received 4 Gy total-body irradiation (200 kV X rays, Xstrahl) to prevent residual murine immune activity against human tumor transplants that might interfere with tumor growth (*16*). After total-body irradiation, prophylactic antibiotics were administered in the drinking water (Ciprofloxacin, 10 mg in 250 ml H_2O) throughout the entire experiment. The radiobiological properties of FaDu tumors *in vivo* are discussed in greater detail by Maftei *et al.* (*17*). These studies were performed in parallel in our research facility.

Monitoring of Tumor Growth

Tumor size was monitored twice per week with diagnostic ultrasound (LOGIQ C5/PRO, 10 MHz linear transducer, GE Healthcare, Germany). Length, width and depth of the tumor were the longest diameters measured in the two planes along and perpendicular to the long axis of the individual tumor. Tumor regression and regrowth were followed until tumors grew to 11–13 mm in maximal diameter; at this time the animals were sacrificed. Tumor volume was calculated according to the ellipsoid volume formula:

$$V = \pi/6 * \text{length} * \text{width} * \text{depth}$$

Tumor volume assessment by ultrasonography had a low intra- and inter-observer variability with a resolution limit of 1 mm^3 (*18*). The tumor volume on the day of irradiation was defined as the initial volume V_0, when the tumors had a length of <8 mm and a depth of 3.7–4.2 mm. The upper limit was chosen in view of the maximal penetration depth of the 23 MeV proton beam used for our experiments, which corresponded to 5 mm. It ensured a tumor depth safety margin of 0.5 mm, taking into account a skin thickness of 0.3 mm.

Photon experiments were conducted 6 months after the proton irradiation. All tumor volumes were measured over a period of 120 days after irradiation or until termination criteria were met i.e., animals were euthanized when the mean diameter of the recurrent tumor exceeded 12–15 mm or when the animal showed signs of pain, distress or suffering. Local control was stated in case of missing tripled volume during observation.

Pulsed and Continuous Proton Irradiation

For a detailed description of the proton irradiation setup, beam preparation, treatment planning and dose verification published previously by Schmid *et al.* see ref. (*13*). In summary, proton irradiation with a single dose of approximately 20 Gy was performed with the ion microprobe SNAKE (Munich tandem accelerator). For pulsed mode a 23 MeV proton beam with 1.3 ns (full width at half maximum) pulse duration focused to ≈100 µm aperture was directed to cover a field of 9 mm diameter by electrical, magnetic and mechanical scanning. The spread-out Bragg peak was realized by using aluminum sheets of 13 different thicknesses. For continuous dose application on a millisecond timescale a beam field of 3×2 mm^2 was prepared and scanned mechanically over the target volume of 9 mm diameter. The total irradiation time in pulsed mode was ≈35 min, and in continuous mode ≈25 min, respectively.

During the irradiation procedure the mice were deeply sedated with ketamine/diazepam (100 mg/kg i.m. | 5 mg/kg i.p.) and the temperature was maintained between 36–37°C by electrically heating the aluminum mouse holder tube. A total number of 12 animals were irradiated in either pulsed or continuous mode.

Mean proton dose was verified for each tumor with a protocol based on Gafchromic™ EBT2 films. The mean tumor dose (± uncertainty) in pulsed mode was 17.4 ± 0.8 Gy and in continuous mode 19.7 ± 1.1 Gy, respectively. Half of the 10% dose deviation between groups resulted from a bigger overlap of the 2×3 mm^2 single fields at the continuous proton irradiation and from one tumor accidentally receiving 22 Gy in this mode. The remaining (unexplained) difference of 5% is assumed to be rooted in the beam current measurement. The absolute dose uncertainty is $<3\%$, which was estimated from calibration curves of the Gafchromic EBT2 films (*13, 19*).

The uncertainty for the mean dose was calculated as the sum of squares of the standard error of the mean dose, the calibration uncertainty and the absolute dose uncertainty.

Photon Reference Irradiation

For the photon reference, the mice were irradiated with a single static field of 1.5×1.5 cm^2 with 6 MV photons from a clinical linear accelerator (Trilogy/Varian, Klinikum rechts der Isar, Technische Universität München). With gantry rotation to 180° the beam entered through the bottom of the cage, where the mice were fixed with the leg extended and the tumor aligned to cross hairs at the cage. Sterile flap

material (Elasto-Gel, Southwest Technologies Inc.) covered the tumor to provide sufficient backscattering.

The beam first traversed solid water (at source–surface distance of 99.3 cm) and the cage wall (2 mm perspex) as build-up material before reaching the tumor, which was positioned in the maximum of the depth dose curve between water-equivalent depths of 14–20 mm (corresponding to 98–100% of the dose maximum). The field was defined by the primary jaws. At a depth of 14 mm, the field size defined by 50% of the nominal dose was 15.0×15.0 mm^2 (measured with Gafchromic EBT2 film), while the aperture of 90% (95%) isodoses was 11.4 mm (10.1 mm). Therefore, the dose to the tumor volume was very homogeneous. The absolute dose varied $\pm 3\%$ (EBT2 films) and the overall uncertainty in absolute dose was estimated to be $\pm 6\%$.

For the dose-response curve with photons, 48 mice were randomized into one of six dose levels (of 0, 10, 15, 20, 30, 40 Gy treating 6, 7, 8, 9, 9, 9 mice, respectively). The treatment time varied between 67 s (10 Gy) and 268 s (40 Gy) at a machine output of 1,000 MU/min (stereotactic radiosurgery mode).

Tumor Growth Delay Determination

Tumor growth delay, (GD) is defined as the difference between the mean time, $t_{3V_0,control}$, nonirradiated tumors needed to triple their volume and the mean time, t_{3V_0}, irradiated tumors needed to reach three times the volume at the time of irradiation, V_0. The growth rate of nonirradiated tumors was determined by fitting each growth curve of the control tumors with an exponential function, $V(t) = V_0 \exp(t/\tau)$. $t_{3V_0,control}$ is given by ln(3) * τ_m, where τ_m is the average of all τ. t_{3V_0} is the average of the times $t_{3V_{0,i}}$ of each tumor i within one dose group. The individual time $t_{3V_{0,i}}$ of each tumor to reach $3V_0$ emerged from linear interpolation of the two points below and above the tripled volume, $3V_0$ (see Fig. 3) and in two cases, by linear extrapolation of the two nearest points below $3V_0$, because the tumor volume reached the abort criterion of 13 mm diameter before the volume $3V_0$ (not observable in the growth curves of Fig. 3). The error of the growth delay ΔGD is calculated by Gaussian error propagation of the statistical errors of $t_{3V_0,control}$ and t_{3V_0}, which are given by the standard error of the mean multiplied with the t factor arising from student t distribution, taking into account that the true mean value is unknown. The errors are given on a 68.3% confidence level.

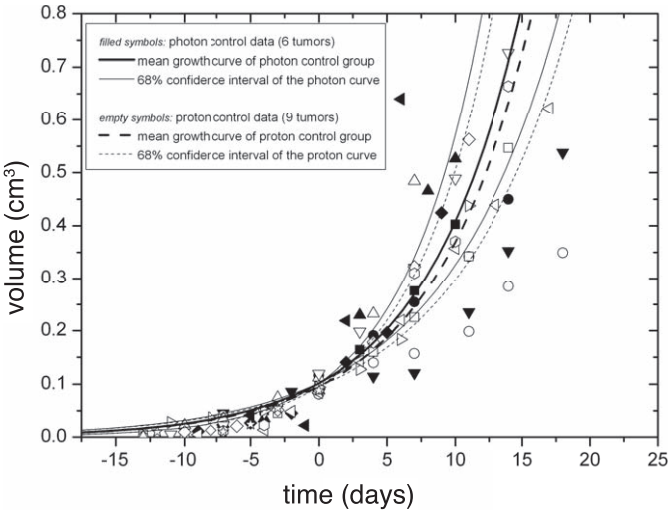

FIG. 1. FaDu tumor growth in nonirradiated control groups as a function of time. The filled symbols mark the control tumor data of the photon irradiation (6 tumors) and the open symbols mark the controls of the proton irradiation (9 tumors). As the aim of the control measurement is to only obtain the growth rate, plotting of time zero for each tumor was set to the time with a tumor volume of approximately 0.1 cm^2. The growth constant of each tumor growth has been fitted with an exponential function (not shown for clarity). Mean tumor growth curves were calculated on the basis of the mean of growth times and displayed with their 68.3% confidence intervals.

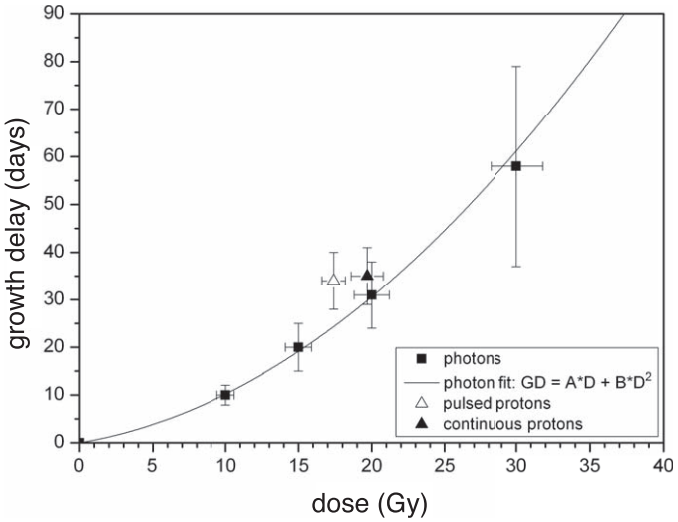

FIG. 2. Tumor growth delay as a function of dose after photon irradiation, as well as after pulsed proton and continuous proton irradiation. The growth delay error bars represent the 68.3% confidence intervals. For proton irradiation the dose error bars are the errors of the reconstructed dose values (0.8 Gy for pulsed and 1.1 Gy for continuous mode) and for photon irradiation the relative dose error of 6% was used.

RBE Calculation and Statistical Analysis

The RBE is defined as the dose ratio of a reference radiation quality (6 MV photons) and the applied radiation (pulsed/continuous protons) to induce the same effect. The dose dependency of growth delay, $GD(D)$, after photon irradiation was fitted by weighted least squares approximation with the following function: $GD(D) = A * D + B * D^2$. The reciprocal variance of the growth delay data points $GD(D_i)$ was used as a weighting factor. The necessary photon dose to induce the certain effect, $D(GD)$, results from inverting the dose effect curve, $GD(D)$. The uncertainty of the RBE, ΔRBE, was calculated by error propagation of the uncertainties of the input parameters growth delay, GD, dose of the pulsed or continuous proton irradiation, D_{Proton}, the fit parameters A, B and the uncertainty of the photon dose calibration, $D(GD)$. As parameters of the fit, A and B were highly correlated, the non-diagonal elements of the covariance matrix were also taken into account.

The growth delay results were evaluated using a nonparametric Mann-Whitney U test or χ^2 test. Differences between groups were considered significant at the confidence level $P \leq 0.05$.

RESULTS

Tumor Growth in Nonirradiated Mice

Nonirradiated FaDu tumors of 9 and 6 control mice from the proton and photon experiments grew with a mean volume doubling time $t_{2V_0} \pm$ SE of 5.2 $\pm$ 0.6 days and 5.0 $\pm$ 0.9 days, respectively. The calculated mean time to triple the volume $V_0 \pm$ SE was 8.2 $\pm$ 0.9 days in the proton control group and 7.9 $\pm$ 1.4 days in the photon control

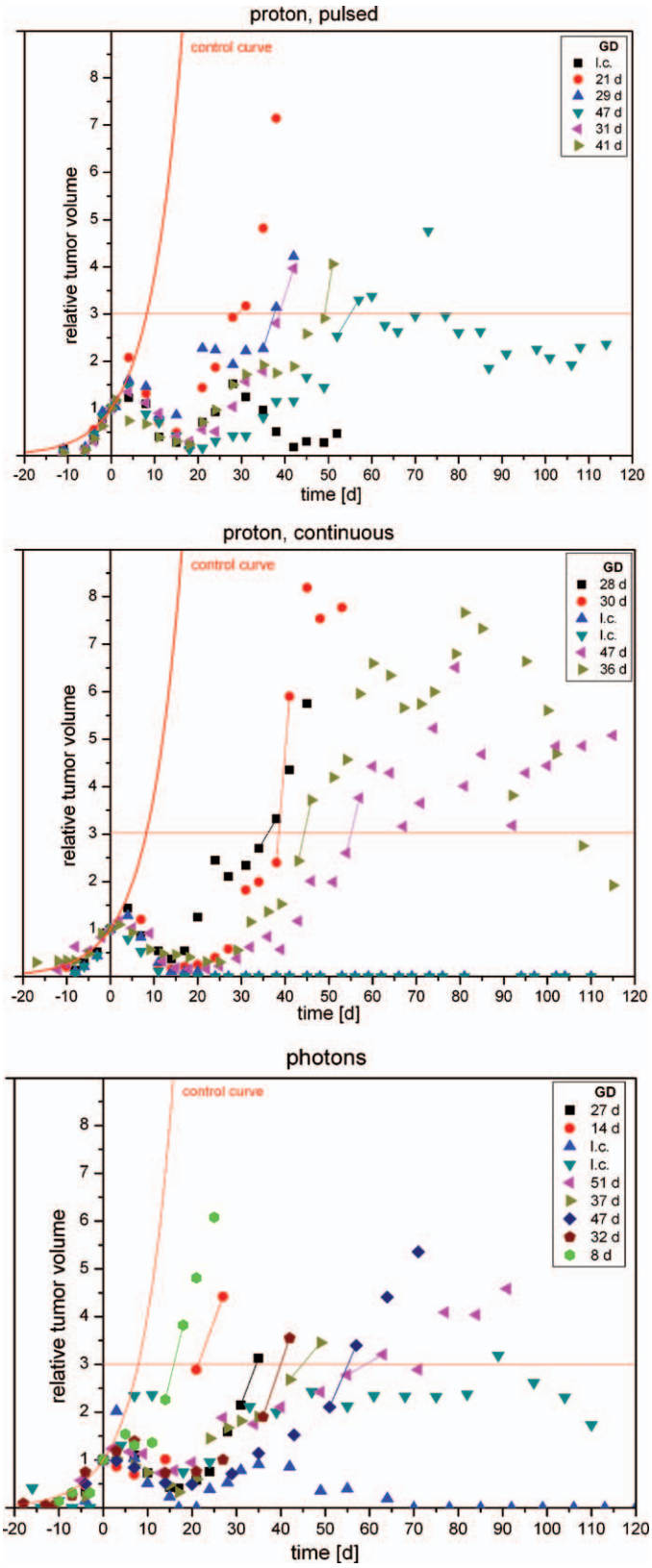

FIG. 3. Tumor regression and regrowth in individual animals after irradiation. Plotted is the tumor volume normalized to the volume at time of irradiation V_0 exposed to (top panel) 17.4 Gy of 23 MeV pulsed protons, (middle panel) 19.7 Gy of 23 MeV continuous protons and (bottom panel) 20 Gy of 6 MV photons. Thin, horizontal red lines mark the tripled tumor volumes, $3V_0$, which are used for the definition of growth delay. Time zero corresponds to the day of irradiation. In figure inset the individual growth delay (GD) of each tumor is given (accounting for the tripling volume time of 8 days for nonirradiated tumors, see red curves). Locally controlled tumors are indicated with ''l.c.''

group. All individual tumor volumes and regression curves are summarized in Fig. 1. No significant differences in tumor growth were observed within the two groups, although the studies were performed in different institutions and at different time points. Due to ultrasonic volumetry and with the use of our validated tumor bank, good experimental reproducibility was achieved.

Tumor Growth Delay in Irradiated Mice and RBE

Results from photon treatments at six different dose levels are shown in Table 1. The tumor growth delay ±SE increased with dose from 12 ± 3 days after application of 10 Gy up to 58 ± 7 days at a dose of 30 Gy. Exposure to 40 Gy resulted in complete local control in all tumors in a follow-up time of 120 days. The growth delay data as a function of dose is plotted in Fig. 2 and was fitted with a polynomial function, $GD(D) = A * D + B * D^2$, resulting in $A = 0.5 \pm 0.5$ day/Gy^{-1} and $B = 0.051 \pm 0.029$ day/Gy^{-2}. The covariance between A and B was determined to be -0.012 d^2/Gy^3.

Pulsed and continuous proton irradiation of tumors resulted in a growth delay ±SE of 34 ± 6 days with 17.4 ± 0.8 Gy and 35 ± 6 days with 19.7 ± 1.1 Gy, respectively (see Table 1 and Fig. 2).

Complete data sets of growth curves for each of the 3 irradiation modes at a dose of approximately 20 Gy are shown in Fig. 3. The measured tumor volumes relative to the initial volume V_0 of individual FaDu tumors after exposure to pulsed protons, continuous protons or 20 Gy photons are plotted against the time after irradiation. Mean tumor volume (±SD) at the day of treatment was 64 ± 26 mm^3 for proton and 83 ± 26 mm^3 for photon experiments. The corresponding mean growth curves for control (nonirradiated) tumors are included in Fig. 3 to allow a direct comparison. The results for mean tumor growth delay ±SE with 34 ± 6 days for pulsed, 35 ± 6 days for continuous protons did not differ significantly from the results for 20 Gy of photon irradiation with 31 ± 7 days. At this dose level, locally controlled tumors occurred with all irradiation types: 1 with pulsed, 2 with continuous protons and 2 with 20 Gy of photons (see Fig. 3: ''local control'').

The RBE was determined by using the dose-effect curve after photon irradiation to compare the effect of pulsed and continuous irradiation on growth delay RBE. The RBE for pulsed protons was 1.22 ± 0.19 and 1.10 ± 0.18 for the continuous irradiation mode. The difference was not statistically significant ($P > 0.05$).

TABLE 1
Results of Tumor Irradiation

Radiation quality	Dose (Gy)	Mice	Locally controlled	GD (days)	V_0 (mm^3)	V_{min}/V_0
Photons, control	0	6	0	-	-	-
Photons	10.0 ± 0.6	7	0	12 ± 3	82 ± 14	1.11 ± 0.20
Photons	15.0 ± 0.9	8	0	20 ± 5	70 ± 18	0.81 ± 0.22
Photons	20.0 ± 1.2	9	2	31 ± 7	90 ± 24	0.67 ± 0.14
Photons	30.0 ± 1.8	9	7	58 ± 7	83 ± 43	0.23 ± 0.15
Photons	40.0 ± 2.4	9	9	-	87 ± 27	-
Protons, control	0	9	0	-	-	-
Protons, pulsed	17.4 ± 0.8	6	1	34 ± 6	78 ± 22	0.21 ± 0.06
Protons, continuous	19.7 ± 1.1	6	2	35 ± 6	50 ± 25	0.25 ± 0.03

Notes. For each radiation quality and dose (± uncertainty), the number of irradiated and number of locally controlled tumors, as well as the mean growth delay (GD) (±SE), initial tumor volume V_0 (±SD), and minimal relative tumor volume (±SE) during follow-up are given.

Minimal Tumor Volume after Irradiation

In some of the tumors proton treatment temporarily induced a complete tumor regression with tumor volumes beyond the resolution of ultrasound measurements. In contrast, tumors treated with 20 Gy of photons never reached these small volumes after irradiation. In Fig. 4, the minimal volumes of tumors—defined as the smallest tumor volume between 1 and 120 days after irradiation normalized to their initial volumes V_0—are plotted as a function of dose. The error bars indicate the 68.3% confidence intervals. It is worth mentioning that within this confidence interval protons were more effective at reducing the tumor volume than photons. The data indicate that ≈30 Gy of photon irradiation were required to provoke the same amount of tumor regression V_{min}/V_0 proton irradiation induced with ≤20 Gy.

DISCUSSION

This current work continues our systematic exploration of the effects of ultra-high dose rates on biological endpoints, *in vivo*. These data are of high relevance for clinical use of laser-accelerated proton beams. Previous experiments on monolayer and 3D tissue cultures (*in vitro*) did not provide evidence for significantly altered radiobiological effectiveness in terms of cytogenetic damage or DNA repair (*8–12*). The RBE values determined for pulsed and continuous irradiation modes were always comparable to the RBE of 1.1, which is achieved by conventional proton therapy (*20*).

Here, we report for the first time on the radiobiological effectiveness of pulsed protons for the treatment of macroscopic tumors *in vivo*. Although the pulsed beam appeared slightly more effective in tumor growth delay, no significant differences to continuous proton beams were observed. With 1.22 ± 0.19 and 1.10 ± 0.18 for pulsed and continuous mode, respectively, the RBE determined for both irradiation modes was also comparable to the RBE of 1.1 of proton irradiation.

For growth delay calculation, only uncontrolled tumors were included. If controlled tumors had been included, with a GD of 120 days – 8 days = 112 days (the maximum observation time was 120 days), the mean growth delay for 17.4 Gy of pulsed and 19.7 Gy of continuous proton irradiation would have been 47 ± 16 days and 61 ± 19 days, respectively, with the corresponding RBEs of 1.21 ± 0.23 and 1.21 ± 0.22, taking into account that the dose-response curve $GD(D)$ is also changed. However, even for this endpoint there would still be no significant difference between the two irradiation modes.

The first radiobiological *in vitro* experiments with laser-driven protons and electrons reveal no differences with respect to the RBE values compared to conventional irradiation sources. Comparing effects of laser-driven 6.5 MeV electrons (0.4–10.2 Gy in 125–4900 pulses of 10^9 Gy/s) with linac-based electron irradiation showed no significant differences in clonogenic cell survival and residual DNA double-strand breaks in cell cultures (*21*). In single-

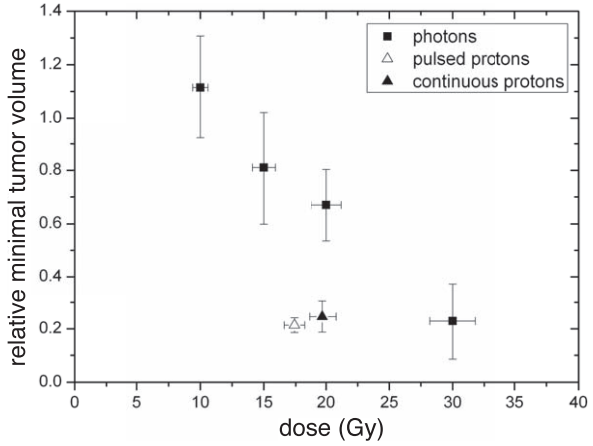

FIG. 4. Mean of minimal tumor volumes of uncontrolled tumors after irradiation normalized to their initial irradiation volumes V_0 as a function of dose. The relative volume error bars represent the 68.3% confidence intervals. After proton irradiation the minimal tumor size is significantly reduced compared to photon irradiation to the same dose.

shot experiments with laser-accelerated 5 MeV protons, we found an RBE of 1.3 ± 0.3 for the induction of DNA damage (γ-H2AX foci 30 min after irradiation) in HeLa cells compared to 200 kV X rays (*7*). The dose rate exceeded 10^9 Gy/s, similar to those used by Doria *et al*. (*22*), who also found similar rates in clonogenic cell survival in V-79 cells compared to conventional sources. The calculated RBE in those experiments was 1.4 ± 0.2 at 10% cell survival in comparison with a 225 kV X-ray source (*22*). In another study, human salivary gland cancer cells were irradiated with doses up to 8 Gy by laser-driven quasi-monoenergetic 2.2 MeV protons, and the RBE for the endpoint of 10% cell survival (colony formation) was 1.20 ± 0.11 (*23*).

Our current *in vivo* experiments in human xenograft tumors show no evidence for a substantially different RBE induced by ultra-high dose rate protons. However, it is important to note that by scanning the beam laterally and in depth in a regular pattern to obtain a homogeneous dose distribution over a volume, in each single tissue voxel several pulses contributed to the total irradiation dose. In addition, our setup the largest contribution of a single pulse was between 1.0–2.5 Gy. It is not expected that, for tumor therapy with a laser-driven proton accelerator in a clinical setup, much higher doses per single pulse will be applied to a tissue voxel. Thus, the used dose delivery seems to be an adequate model for investigating the effectiveness of pulsed dose deposition in radiation therapy.

It has been proposed that ultra-high dose rate irradiation might lead to oxygen depletion in conventional irradiation modes (X ray and electrons) (*24*). It is possible that this, oxygen depletion might negatively influence the radiosensitivity of tumors and thus, might reduce tumor control since hypoxic tumors are in general more radioresistant than normoxic tumors. However, for pulsed proton beams the impact of oxygen depletion on radioresistance has not yet been elucidated. The investigation of tumor hypoxia following ultra-high dose rate irradiation was not evaluated in the present study.

It must be noted that in our experiments only one tumor type (FaDu) was used; different tumor volumes and/or hypoxia status as well as tumor type may influence the radiobiological effectiveness of ultra-high dose rate irradiation. However, based on our previous *in vitro* experiments (*8–12*) we do not expect a relevant difference between pulsed and conventional proton irradiation.

CONCLUSIONS

Our *in vitro* and *in vivo* studies showed no evidence of a substantially different radiobiology associated with the ultra-high dose rate that characterizes protons generated from advanced laser technology. Our results are consistent with the available literature, which shows that the RBE for pulsed protons is likely to be similar to the known effectiveness of conventional proton beams. Our experiments have also shown that protons were more effective in the reduction of tumor volume than photons at the same dose. We conclude that dose prescription for pulsed protons can be based on established therapeutic concepts for protons. However, one should bear in mind that differences in the RBE values smaller than 10% cannot be excluded yet and should be accounted for in dose constraints for organs at risk.

ACKNOWLEDGMENTS

This work was supported by the DFG-Cluster of Excellence ''Munich-Centre for Advanced Photonics'' and by the Maier-Leibnitz Laboratory, Munich.

Received: July 8, 2013; accepted: October 23, 2013; published online: February 13, 2014

REFERENCES

1. Durante M, Loeffler JS. Charged particles in radiation oncology. Nat Rev Clin Oncol 2010; 7:37–43.
2. Linz U, Alonso J. What will it take for laser driven proton accelerators to be applied to tumor therapy? Phys Rev St Accel Beams; 2007; 10:1–8.
3. Steinke S, Henig A, Schnürer M, Sokollik T, Nickles P V, Jung D, et al. Efficient ion acceleration by collective laser-driven electron dynamics with ultra-thin foil targets. Laser Part Beams 2010; 28:215–21.
4. Tajima T. Laser acceleration and its future. Proc Jpn Acad Ser B Phys Biol Sci 2010; 86:147–57.
5. Hofmann KM, Schell S, Wilkens JJ. Laser-driven beam lines for delivering intensity modulated radiation therapy with particle beams. J Biophotonics 2012; 5:903–11.
6. Bin J, Allinger K, Assmann W, Dollinger G, Drexler GA, Friedl AA, et al. A laser-driven nanosecond proton source for radiobiological studies. Appl Phys Lett 2012; 101:243701.
7. Dollinger G, Bergmaier A, Hable V, Hertenberger R, Greubel C, Hauptner A, et al. Nanosecond pulsed proton microbeam. Nucl Instr and Meth 2009; B 267:2008–12.
8. Auer S, Hable V, Greubel C, Drexler G, Schmid T, Belka C, et al. Survival of tumor cells after proton irradiation with ultra-high dose rates. Radiat Oncol 2011; 6:139.
9. Schmid TE, Dollinger G, Hable V, Greubel C, Zlobinskaya O, Michalski D, et al. The effectiveness of 20 MeV protons at nanosecond pulse lengths in producing chromosome aberrations in human-hamster hybrid cells. Radiat Res 2011; 175:719–27.
10. Schmid TE, Dollinger G, Hauptner A, Hable V, Greubel C, Auer S, et al. No Evidence for a Different RBE between Pulsed and Continuous 20 MeV Protons. Radiat Res 2009; 172:567–74.
11. Zlobinskaya O, Dollinger G, Michalski D, Hable V, Greubel C, Du G, et al. Induction and repair of DNA double-strand breaks assessed by gamma-H2AX foci after irradiation with pulsed or continuous proton beams. Radiat Environ Biophys 2012; 51:23–32.
12. Schmid TE, Dollinger G, Hable V, Greubel C, Zlobinskaya O, Michalski D, et al. Relative biological effectiveness of pulsed and continuous 20 MeV protons for micronucleus induction in 3D human reconstructed skin tissue. Radiother Oncol 2010; 95:66–72.
13. Greubel C, Assmann W, Burgdorf C, Dollinger G, Du G, Hable V, et al. Scanning irradiation device for mice in vivo with pulsed and continuous proton beams. Radiat Environ Biophys 2011; 50:339–44.
14. Bayer C, Schilling D, Hoetzel J, Egermann HP, Zips D, Yaromina A, et al. PAI-1 levels predict response to fractionated irradiation in

10 human squamous cell carcinoma lines of the head and neck. Radiother Oncol 2008; 86:361–8.

15. Krause M, Hessel F, Zips D, Hilberg F, Baumann M. Adjuvant inhibition of the epidermal growth factor receptor after fractionated irradiation of FaDu human squamous cell carcinoma. Radiother Oncol 2004; 72:95–101.

16. Teicher BA. Tumor models in cancer research. Humana Press; 2002. p. 690.

17. Maftei C-A, Bayer C, Shi K, Vaupel P. Intra- and intertumor heterogeneities in total, chronic, and acute hypoxia in xenografted squamous cell carcinomas. Detection and quantification using (immuno)fluorescence techniques. Strahlenther Onkol 2012; 188:606–15.

18. Ayers GD, McKinley ET, Zhao P, Fritz JM, Metry RE, Deal BC, et al. Volume of preclinical xenograft tumors is more accurately assessed by ultrasound imaging than manual caliper measurements. J Ultrasound Med 2010; 29:891–901.

19. Reinhardt S, Hillbrand M, Wilkens JJ, Assmann W. Comparison of Gafchromic EBT2 and EBT3 films for clinical photon and proton beams. Med Phys 2012; 39:5257–62.

20. Paganetti H, Niemierko A, Ancukiewicz M, Gerweck LE, Goitein M, Loeffler JS, et al. Relative biological effectiveness (RBE) values for proton beam therapy. Int J Radiat Oncol Biol Phys 2002; 53:407–21.

21. Laschinsky L, Baumann M, Beyreuther E, Enghardt W, Kaluza M, Karsch L, et al. Radiobiological effectiveness of laser accelerated electrons in comparison to electron beams from a conventional linear accelerator. J Radiat Res 2012; 53:395–403.

22. Doria D, Kakolee KF, Kar S, Litt SK, Fiorini F, Ahmed H, et al. Biological effectiveness on live cells of laser driven protons at dose rates exceeding 109 Gy/s. AIP Advances 2012; 2:11209.

23. Yogo A, Daido H, Bulanov S V, Nemoto K, Oishi Y, Nayuki T, et al. Measurement of relative biological effectiveness of protons in human cancer cells using a laser-driven quasimonoenergetic proton beamline. Appl Phys Lett 2011; 98:53701.

24. Wilson P, Jones B, Yokoi T, Hill M, Vojnovic B. Revisiting the ultra-high dose rate effect: implications for charged particle radiotherapy using protons and light ions. Br J Radiol 2012; 85:933–9.